Andean Geology 41 (2): 293-313. May, 2014
doi: 10.5027/andgeoV41n2-a02

Andean Geology
formerly Revista Geológica de Chile
www.andeangeology.cl

Basement geometry and sediment thickness of Lago Fagnano (Tierra del Fuego)

Federico Damián Esteban[1], *Alejandro Tassone[1], Emanuele Lodolo[2], Marco Menichetti[3], Horacio Lippai[1], Nicolas Waldmann[4], Alexia Darbo[2], Luca Baradello[2], Juan F. Vilas[1]

[1] *CONICET-Instituto de Geociencias Básicas, Ambientales y Aplicadas (IGeBA), Departamento de Ciencias Geológicas, Facultad de Ciencias Exactas y Naturales, Universidad de Buenos Aires, Ciudad Universitaria C1428EHA, Buenos Aires, Argentina. esteban@gl.fcen.uba.ar; atassone@gl.fcen.uba.ar; lippai@gl.fcen.uba.ar; vilas@gl.fcen.uba.ar*

[2] *Istituto Nazionale di Oceanografia e di Geofisica Sperimentale (OGS), Borgo Grotta Gigante 42 /C, Sgonico, Trieste, 34010, Italy. elodolo@ogs.trieste.it; lbaradello@ogs.trieste.it*

[3] *Dipartimento di Scienze della Terra, Vita e dell'Ambiente dell'Università di Urbino Campus Scientifico 'E. Mattei' 61020 Urbino (PU), Italy.*
marco.menichetti@uniurb.it

[4] *Department of Marine Geosciences, University of Haifa, Mt. Carmel, 31905, Haifa, Israel.*
nwaldmann@univ.haifa.ac.il

* *Corresponding author: atassone@gl.fcen.uba.ar*

ABSTRACT. Lago Fagnano, an E-W elongated basin located in the central part of Isla Grande de Tierra del Fuego, occupies a structural depression originated along a segment of the Magallanes-Fagnano fault system. Its evolution was mostly conditioned by tectonic processes, and later was affected by glacial and glacio-lacustrine depositional events. New high-resolution single-channel seismic data, integrated with previous seismic profiles, and geological information acquired in the surroundings of the Lago Fagnano, allows us reconstructing the basement surface of the lake, and the geometry, distribution, and thickness of the glacial and glacio-lacustrine sequences. We recognized three main sub-basins within the Lago Fagnano: **1.** a medium-size (*ca.* 21x5 km), deep (373 m), and asymmetric basin to the east; **2.** an E-W trending (44x3 km), shallower (150 m) central sub-basin; and **3.** a smaller (3.5x1.3 km), shallow (128 m) sub-basin to the west. The isopach sediment map shows that the most pronounced deposition occurred along the E-W axis of the lake, with a gradual increase in thickness towards east (from 100 to 150 m). The glacial deposits are widespread along the basin. The lacustrine sediments are preferentially localized along the E-W axis of the lake filling topographic lows. The shape of the sub-basins and their location in relation with the Magallanes-Fagnano fault system, along with the distribution, geometry, and thickness of the sedimentary units, show that the general morphology of the Lago Fagnano was mostly controlled by pre-existing and syntectonic features. Based on the structural data observed in the outcrops around the Lago Fagnano and the geophysical data, we proposed that the lake is composed by 4 amalgamated pull-apart sub-basins.

Keywords: Tierra del Fuego, Lago Fagnano, Magallanes-Fagnano Fault System, Single-channel Seismic Profiles, Basement geometry, Sedimentary cover.

RESUMEN. Geometría del basamento y espesores sedimentarios del lago Fagnano (Tierra del Fuego). El lago Fagnano, una cuenca elongada E-W en la parte central de la isla Grande de Tierra del Fuego, ocupa una depresión estructural originada a lo largo de un segmento del sistema de fallas Magallanes-Fagnano. Su evolución estuvo principalmente condicionada por procesos tectónicos y, luego, fue afectada por eventos deposicionales glaciales y glaciolacustres. Nueva sísmica monocanal de alta resolución, integrada con perfiles sísmicos previos e información geológica adquirida en los alrededores del lago Fagnano, nos permite reconstruir la superficie del basamento del lago, y las geometrías y espesores de las secuencias glaciales y glaciolacustres. Reconocimos tres subcuencas principales dentro del Lago Fagnano: **1.** una subcuenca asimétrica profunda (373 m) de tamaño medio (*ca.* 21x5 km) en el este; **2.** una gran subcuenca central (44x3 km) más somera (150 m); y **3.** una pequeña subcuenca occidental (3,5x1,3 km) somera (128 m). El mapa isopáquico muestra que los mayores depósitos se localizan a lo largo del eje E-W del lago, con un incremento gradual del espesor hacia el este (de 100 a 150 m). Los depósitos glaciales están ampliamente distribuidos a lo largo de la cuenca. Los sedimentos lacustres están preferentemente localizados a lo largo del eje E-W rellenando los bajos topográficos. La forma de las subcuencas y su localización en relación con el Sistema de Fallas Magallanes-Fagnano, junto con la distribución, geometría y espesor sedimentario de las unidades sedimentarias, muestra que la morfología general del lago Fagnano estuvo principalmente controlada por características tectónicas preexistentes y por fallas sintectónicas. Basándonos en los datos estructurales en los alrededores del lago Fagnano y en los datos geofísicos, proponemos que el lago está compuesto por 4 subcuencas de 'pull aparts' amalgamadas.

Palabras clave: Tierra del Fuego, Lago Fagnano, Sistema de Fallas Magallanes-Fagnano, Sísmica monocanal, Geometría del basamento, Cobertura sedimentaria.

1. Introduction

Lago Fagnano (LF; or Lago Khami, as originally called by the native inhabitants) is located in the central part of Isla Grande de Tierra del Fuego (TdF; Fig. 1). It occupies part of the tectonic depression originated by a segment of the South America-Scotia transform boundary, which traverses broadly E-W the TdF region (Fuenzalida, 1972; Dalziel, 1989; Lodolo *et al.,* 2003). The lake has an area of 587 km^2 and it extends over than 100 km, with an average width of 6 km.

Since the late Pleistocene, a glacier originating from the Cordillera Darwin, has expanded eastwards through this tectonic depression now occupied by the lake, with its external front reaching a maximum advance identified at about 35-40 km east of the present-day eastern shore (Caldenius, 1932). Glacial sediments accumulated during the entire Holocene, and may date back to the Last Glacial Maximum (Coronato *et al.,* 2009; Rabassa *et al.,* 2011).

In the last ten years, a series of geophysical and geological surveys have been conducted in the TdF region, focusing primarily in the tectonic evolution of the South America-Scotia plate during the Cenozoic, and analyzing the features associated with this transform margin (Esteban *et al.,* 2011; Lippai *et al.,* 2004; Lodolo *et al.,* 2003, 2007; Menichetti *et al.,* 2001, 2007a and b, 2008; Tassone *et al.,* 2005, 2011; Waldmann *et al.* 2008, 2009, 2010a and b). As a result, the bathymetry of the lake, its glacio-lacustrine deposits, and the main tectonic mechanisms that produced the depression have been widely studied.

In this work, seismic profiles were used to reconstruct the basement surface of LF, and the geometry and thickness of glacial and glacio-lacustrine sequences. This information was then used to analyze the relationship between pre-existing tectonic structures and depositional events in this sector of the TdF region. The results were integrated with previous data from the lake itself and the surrounding areas. Finally a model for the origin of LF is proposed in the frame of the TdF Cenozoic evolution.

2. Regional geological and morphological setting of the Lago Fagnano

2.1. Main structural lineaments

During the Cenozoic, the southernmost region of the Isla Grande del Tierra del Fuego was affected by a left-lateral strike-slip tectonics (Cunningham, 1993, 1995). The wrench faults are overprinted on compressional structures of the late Cretaceous Andean orogeny (Fig. 2). The nature of the strike slip tectonics is mainly transtensional with the development of extensional faults and the formation of pull-apart basins along the main master faults. These basins are known along the entire segment for more than 600 km from the Pacific Ocean through

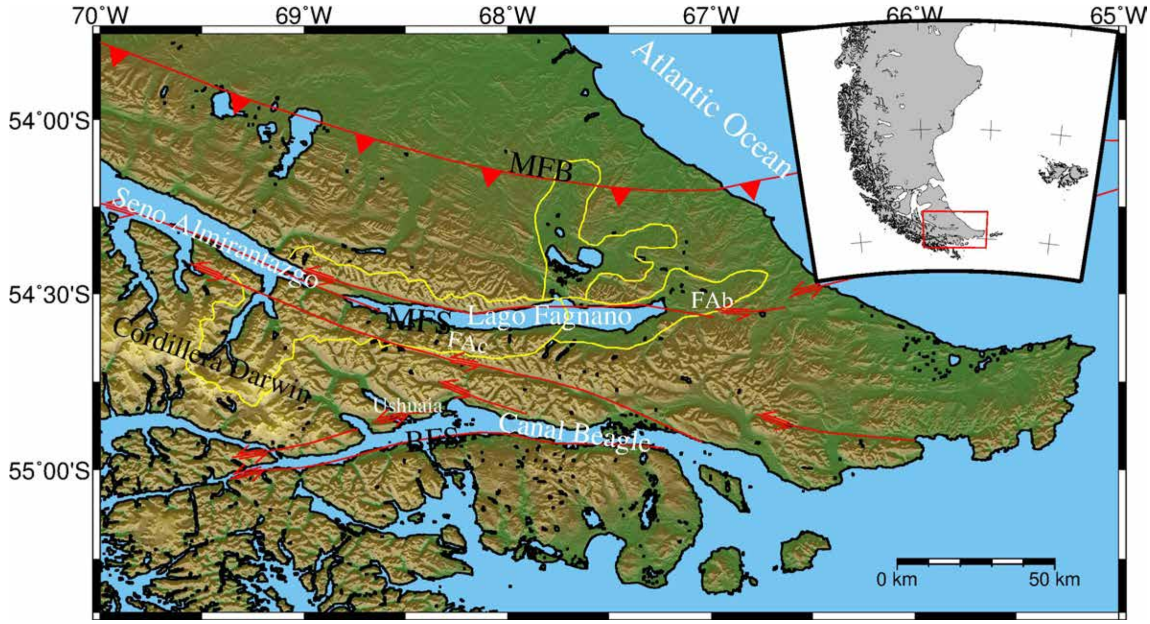

FIG. 1. Location map of the Lago Fagnano in the Isla Grande de Tierra del Fuego (TdF). **MFB:** Magallanes Fold-Thrust Belt; **MFS:** Magallanes-Fagnano Fault System; **BFS:** Beagle Fault System; **FAc:** Fagnano Glacier Accumulation Area; **FAb:** Fagnano Glacier Ablation Area. Glacier areas and fronts have been taken from Coronato *et al.* (2009). Inset map shows studied area in South America.

the Magallanes Strait, the Seno Almirantazgo, the LF, to the Atlantic off-shore (Fuenzalida, 1972; Dalziel, 1989; Lodolo *et al.,* 2003; Menichetti *et al.,* 2008; Tassone *et al.,* 2011). LF occupies the central segment of the MFS for a length of more than 100 km with a E-W strike (Klepeis, 1994; Lodolo *et al.,* 2002a, 2003). The structures of the LF area have been affected by two tectonic phases: **(I)** the Late Cretaceous Andean compressional phase with a prevalent ductile deformation, and **(II)** the Oligocene-Quaternary strike-slip phase where the deformation is essentially brittle (Menichetti *et al.,* 2008; Esteban *et al.,* 2009, 2011). The compressional phase (I) is represented by a few basement wedges that were uplifted and thrusted towards the N and the N-E in complex slices with sole thrusts propagating in- or out-of sequence with a stepped thrust geometry running from the deep internal basement roots to the shallow stratigraphic levels of the foreland (Fig. 2; Menichetti *et al.,* 2008).

One of these basement wedges is located at the boundary between Sierra Valdivesio and Sierra Alvear thrusts sheets where the Upper Jurassic to Lower Cretaceous metasediments are involved in the ductile deformation. NE of the Sierra de Las Pinturas is located the leading edge of the main thrust front of the Fuegian Andes (Fig. 2).

Several Late Cretaceous shoshonitic plutons (Cerro Kranck and Cerro Jeu Jepen; Fig. 2) are emplaced in the central and the eastern sectors of the LF (Cerredo *et al.,* 2005, 2011; Peroni *et al.,* 2008). The shape of these structures and the relationship with the host rocks are well documented with the field data as well as with geophysical surveys (Peroni *et al.,* 2008).

In the phase (II) the wrench tectonics overprinted the Andean structures with a complex array of left-lateral, E-W subvertical strike-slip faults that shaped the LF. The main structures are represented by the Hope-Catamarca-Knokeke fault, the Río Turbio-Las Pinturas fault, and San Rafael fault (Figs. 2 and 3; Menichetti *et al.,* 2008). Subsidiary to these structures are several transtensional faults that subdivide the main segments in shorter arrays.

The E-W striking, subvertical Hope-Catamarca-Knokeke represents a main array of the principal deformation zone crossing LF. In the western sector, this fault strikes W-NW to NW and affects the Lemaire Formation (Upper Jurassic; Fig. 3A). South of Sierra Beauvoir, the fault is sub-vertical and dips south with subhorizontal striae (Fig. 3B). The fault crosses the lake in the central sector reaching the southeastern shore where it is buried by the glacial sediments and connects with the array in the Sierra Lucas Bridge, located eastward.

The San Rafael fault runs north of Sierra Valdivieso and forms a complex array of steeply north dipping WNW-ESE striking fault systems that affect the Lemaire Formation (Upper Jurassic, Fig. 3E). Las Pinturas fault in the NE and the San Rafael fault in the SW represent two E-W structures associated with the master faults of the Hope-Catamarca-Knokeke system. Both faults run roughly parallel to the lake shore forming a releasing step-over and develop secondary transversal extensional structures. The kinematics of these two subvertical E-W faults is mainly strike-slip, while for the Hope-Catamarca-Knokeke the extensional component is larger. The Río Turbio-Las Pinturas fault array is located along the northern shore of LF (Fig. 2). Both present a sub-vertical plane striking E-W. Sub-horizontal striae on the fault plane suggest a dominant strike-slip kinematics with a significant normal component (Fig. 3C and D). In the easternmost tip of the LF, this fault affects fluvioglacial deposits (Fig. 3C) highlighting a Quaternary activity. Recent GPS analysis (Mendoza *et al.,* 2011) in the Argentinean side of Tierra del Fuego Island shows that the MFS over the LF accommodates the horizontal deformation with an average slip of 4 mm/yr (Mendoza, 2008; Mendoza *et al.,* 2010, 2011).

The eastern sector of the LF has a minor uplift of 0.2 mm/yr (± 0.2), while the western sector is affected by an absolute uplift of 3.3 mm/yr (±0.3) and a N-S shortening. This difference seems to be associated to neotectonics with minor contribution due to regional glacial isostatic adjustment (Mendoza *et al.,* 2011).

In Tierra del Fuego, there are a set of regional secondary fault zones, which strike NNW-SSE and apparently underwent a right lateral offset of about 20 km from Middle Eocene to Miocene times (Rossello, 2005). This author describes them as parts of an early single anti-Riedel fault. In the Lago Fagnano area, these secondary fault zones are present in the Río Claro area and in the SW shore of LF.

2.2. Simplified stratigraphic setting

The geological units surrounding the LF span from Jurassic-Cretaceous rocks of the Rocas Verdes basin (Lemaire, Beauvoir and Yahgán formations), through the Cenozoic sediments of the Magallanes foredeep to Quaternary deposits (Fig. 2; Menichetti *et al.,* 2007a). The Cerro Hope, Sierra Valdivieso and Sierra Alvear, located to the west and to the south of LF, respectively (Fig. 2), correspond to the upper Jurassic Lemaire Formation (Borrello, 1969), which is composed of rhyolitic and dacitic lava and tuffs, frequently of ignimbrite type, with sandy and sometimes conglomeratic inter-bedding (Caminos *et al.,* 1981). Towards the northwest, in the Sierra Beauvoir (or Inju Gooiyin) the Lower Cretaceous Beauvoir Formation outcrops (Camacho, 1967), which is composed of dark mudstones, shales and tuffs, with intercalations of fine sandstones and layers of marl (Menichetti *et al.,* 2007a). Sierra Las Pinturas, located to the NE, is composed of yellowish grey, fine-to-very fine sandstones, with intercalations of shelly limestones, mudstones and conglomerates, belonging to the lower Paleogene Río Claro Formation (Camacho, 1967). In addition to the formations described, there are two upper Cenozoic plutonics bodies outcropping around the LF, the Cerro Kranck to the north, and Cerro Jeu Jepen to the SE (Fig. 2), which are composed of syenites, gabbros and monzodiorites (Tassone *et al.,* 2005; Peroni *et al.,* 2007; Cerredo *et al.,* 2011). The lowlands around LF are characterized by Quaternary fluvial, glacio-fluvial and glacial deposits. Along the NW and mainly the SE to E shores of LF, different types of moraines have been recognized by Coronato *et al.* (2009). The fluvial and glacio-fluvial deposits are related to the main rivers (Río Claro, Río Turbio) that flow towards the lake (Fig. 2; Menichetti *et al.,* 2007a). In a general manner, the mountain ranges surrounding the LF are composed of Mesozoic metasediments and plutonic rocks, while the lowlands correspond to Quaternary sediments.

2.3. Lago Fagnano bathymetry

The bathymetric map of the LF allows recognizing the main morpho-bathymetric features (Fig. 4; Lodolo *et al.,* 2002b; Lippai *et al.,* 2004; Zanolla *et al.,* 2011). The lake floor is divided into three depocenters of different water depths: eastern, central and western. The first two are separated by a morphologically complex, shallow relief located in the central part of the lake in correspondence with the Río Claro outlet. The relatively smaller eastern main depocenter (*ca.* 24x5 km) is characterized by

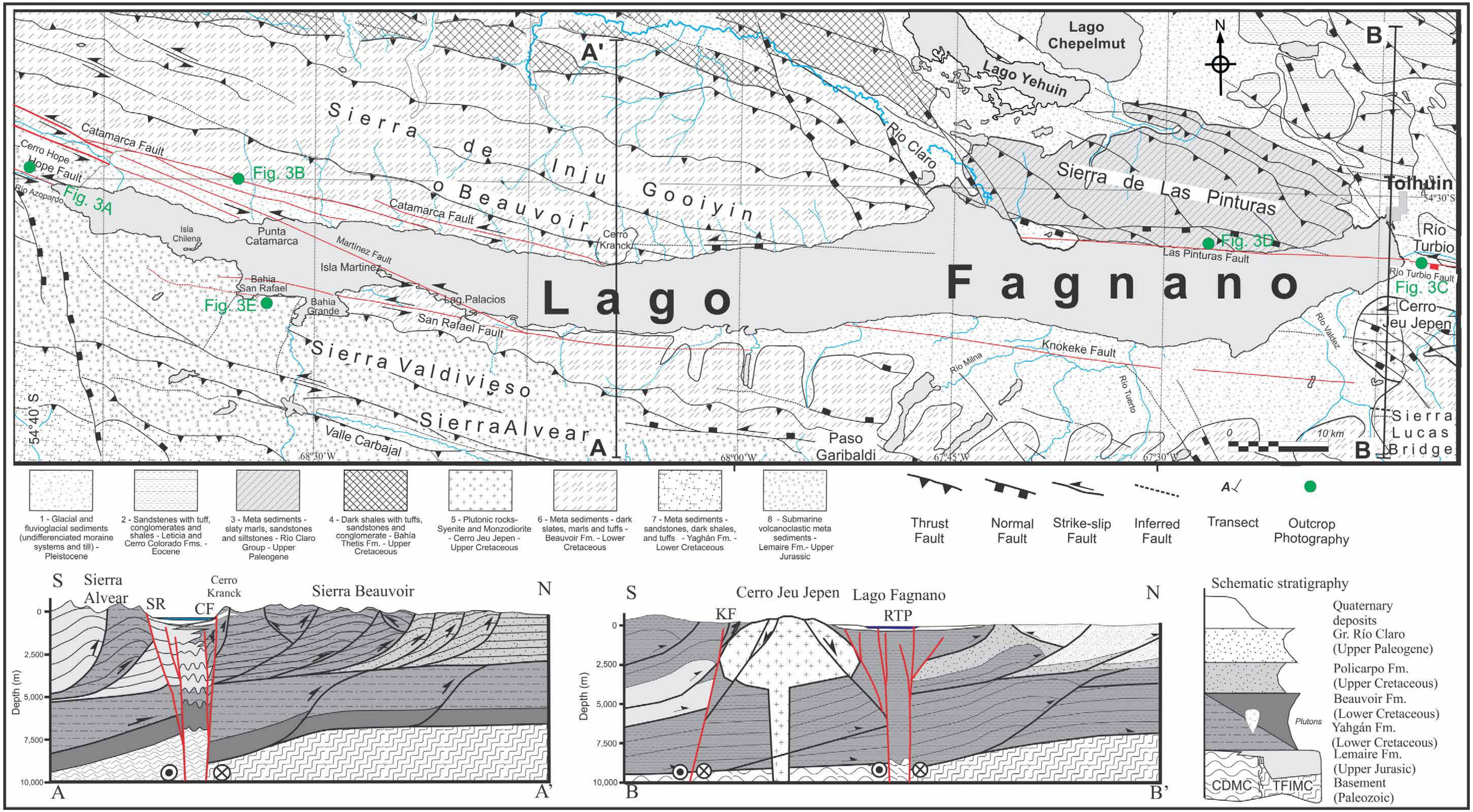

FIG. 2. Geological map of the Lago Fagnano area and geological cross sections with a schematic stratigraphy (adapted from Peroni, 2012). In red are shown the main transcurrent faults associated with the Magallanes-Fagnano Fault system. **CF:** Catamarca fault. **KF:** Knokeke fault; **RTP:** Río Turbio-Las Pinturas fault. **SR:** San Rafael fault; **CDMC:** Cordillera Darwin Metamorphic Complex; **TFIMC:** Tierra del Fuego Igneous and Metamorphic Complex.

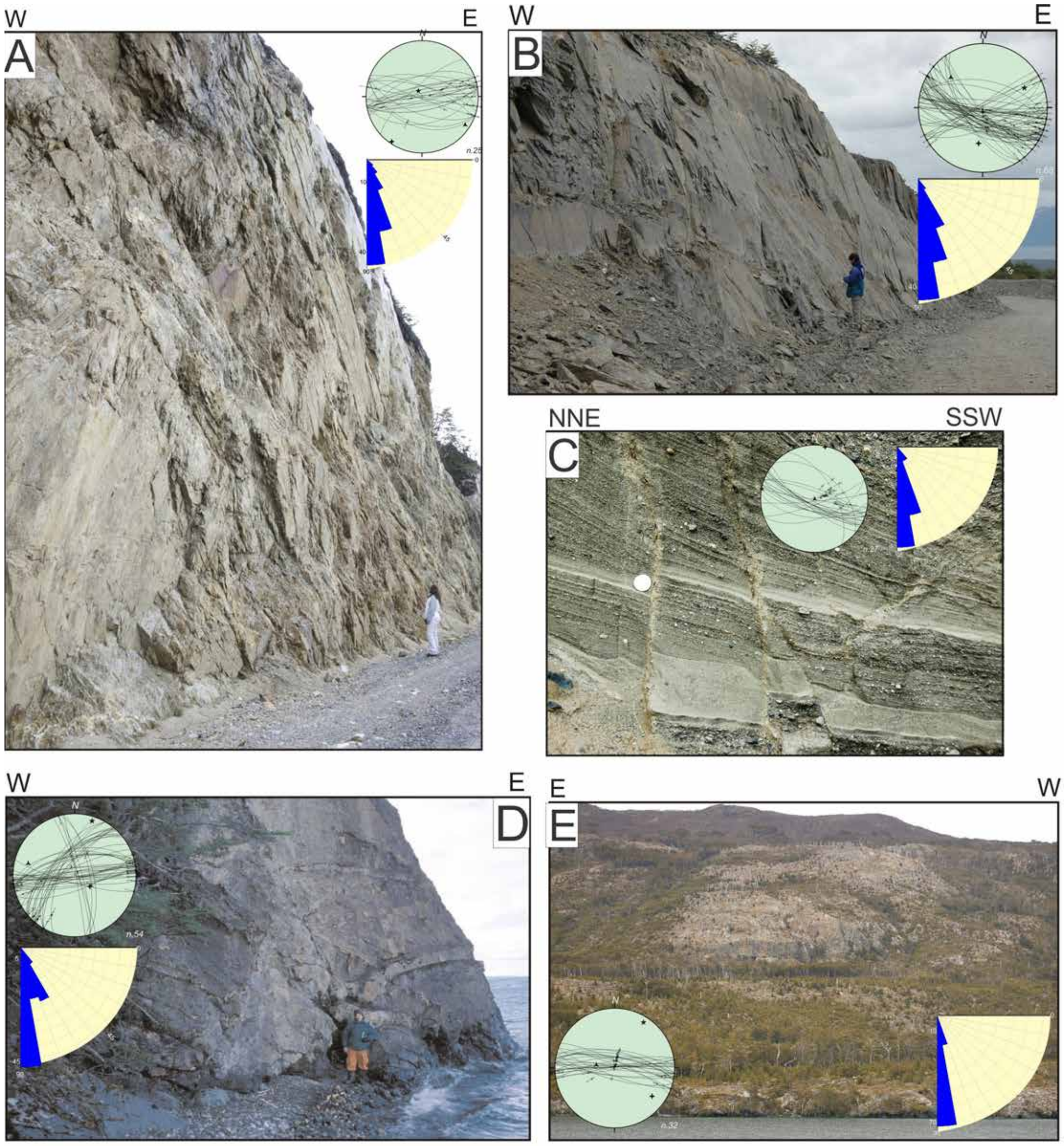

FIG. 3. Photographs and structural data of the main faults in the Lago Fagnano area. Summary of the lower hemisphere equal area plots of the main fault planes associated with the lineaments. Kamb contours every 2 sigma of the fault planes with slickenlines; orientation of the main stress axes (sigma 1 - triangle, sigma 2 - cross, sigma 3 - star) calculated with the Angelier inversion method (Angelier and Goguel, 1979). Number (n) of measurements is indicated for each structural population. **A.** Hope fault in Lemaire Formation (Upper Jurassic); **B.** Catamarca fault in Beauvoir Formation (Lower Cretaceous); **C.** Río Turbio fault in glacifluvial deposits (Quaternary); **D.** Las Pinturas fault in Río Claro Group (Upper Paleogene); **E.** San Rafael fault in Lemaire Formation (Upper Jurassic). See location in figure 2 and 5.

the maximum water depth (206 m) and a peculiar asymmetric shape with steeper slopes towards the northern shore of the lake and gently towards the south. Instead, in the central main depocenter (*ca.* 58x5 km) the water depth does not exceed 165 m and the shape is broadly symmetric. Both basins present a relatively flat depocentral area (Zanolla *et al.,* 2011). These two sectors are thought to correspond to at least two pull-apart basins, formed along the MFS (Lodolo *et al.,* 2003, 2007; Tassone *et al.,* 2005; Menichetti *et al.,* 2008; Zanolla *et al.,* 2011). Two relative Bouguer gravity minima which

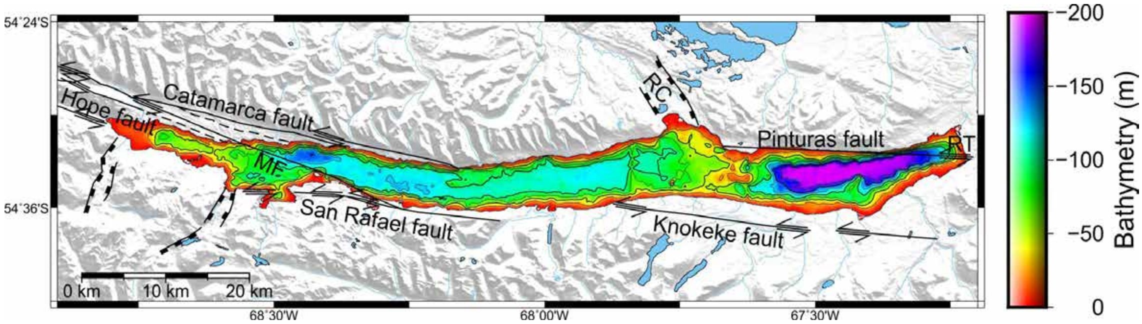

FIG. 4. Simplified bathymetric map of the Lago Fagnano. Depth measured below mean lake water level. The Digital Terrain Model (DTM) of the surroundings has been taken from SRTM v. 4.1 (Farr *et al.,* 2007). Major faults are indicated in black. Locations in figure 5. **MF:** Martínez fault; **RT:** Río Turbio fault; **RC:** Río Claro fault.

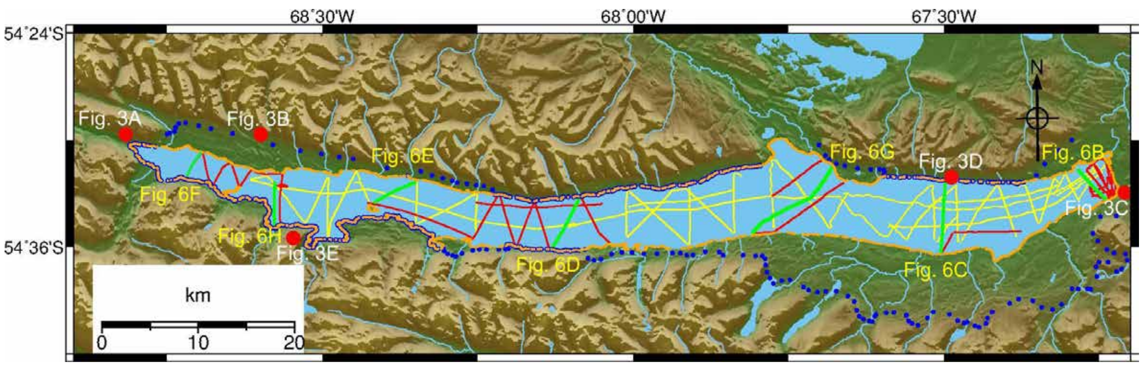

FIG. 5. Seismic position map of the high-resolution profiles acquired in March 2009 (red lines), and profiles (yellow lines) acquired by Waldmann (2008). Numbered green lines are the profiles shown in figure 6. Red dots indicate the photographs location of figure 3. Blue and orange dots correspond to the data off the LF shoreline (limit of the Quaternary glacial deposits and Mesozoic rocks) used to generate the top glacial surfaces and the top basement grids within Lago Fagnano, respectively, following the correlation of the seismostratigraphic and geologic units. See text for details.

are aligned broadly E-W with the depocenters support this interpretation (Lodolo *et al.,* 2007). The western depocenter is smaller (*ca.* 5x2 km) with a maximum depth of about 80 m is found at the western tip of LF.

2.4. Glacial history

The glacial landforms around LF are mainly related to the Upper Pleistocene glaciations, when the glaciers spread from the Cordillera Darwin ice sheet, and flowed to the east (Caldenius, 1932; Bujalesky *et al.,* 1997). During the Last Glacial Maximum, *ca.* 25 ka (calibrated before present; Rabassa *et al.,* 2011), the glacier developed in a relatively narrow zone, within an alpine-type landscape with almost 50 alpine-type glaciers tributaries flowing from the northern and southern sides (Rabassa *et al.,* 2011). This glaciation covered an area of ~4,000 km^2 and its front extended 35 km eastward of the present day lake coast (Fig. 1, Coronato *et al.,* 2009). The glacial accumulation of the Fagnano glacier in the Last Glacial Maximum extended just to the present Río Claro outlet. At least three ice-tongues spread from the accumulation zone towards north and northeast, and eastwards to the LF eastern sector (Fig. 1, Coronato *et al.,* 2009).

During the Late Glacial (18 to ~12 ka), there was a general glacial retreat that affected the Fagnano glacier and the southern Patagonia (Heusser, 1998; Sugden *et al.,* 2005). Despite the general withdrawal, a succession of higher-humidity short periods caused glaciers re-advances (Waldmann *et al.,* 2010a). At least, four recessional phases have been recognized

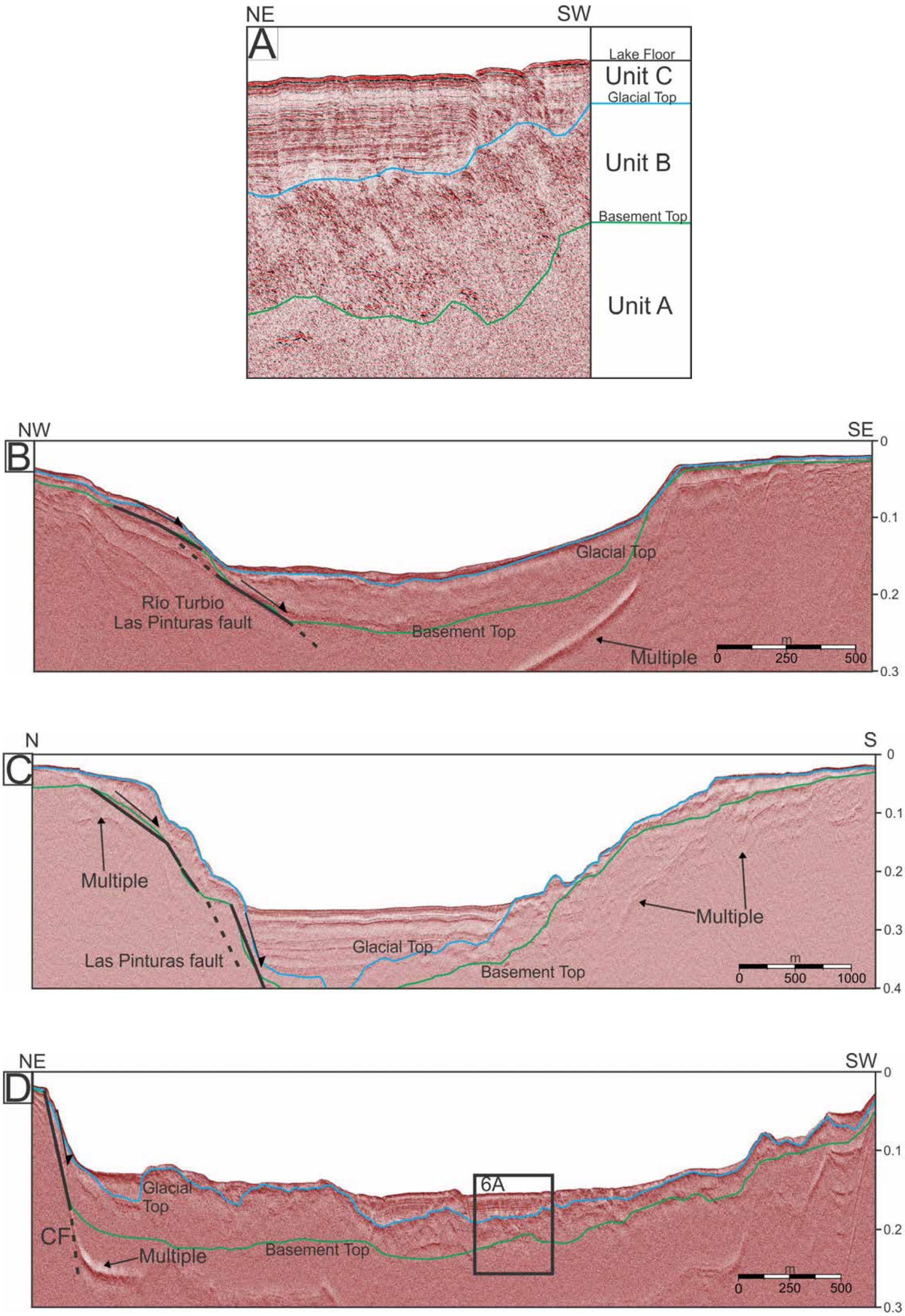
NE
SW
A
Lake Floor
Unit C
Glacial Top
Unit B
Basement Top
Unit A
NW
SE
B
Glacial Top
Río Turbio
Las Pinturas fault
Basement Top
Multiple
m
0 250 500
0
0.1
0.2
0.3
TWT (s)
N
S
C
Multiple
Glacial Top
Las Pinturas fault
Basement Top
Multiple
m
0 500 1000
0
0.1
0.2
0.3
0.4
TWT (s)
NE
SW
D
Glacial Top
6A
CF
Multiple
Basement Top
m
0 250 500
0
0.1
0.2
0.3
TWT (s)

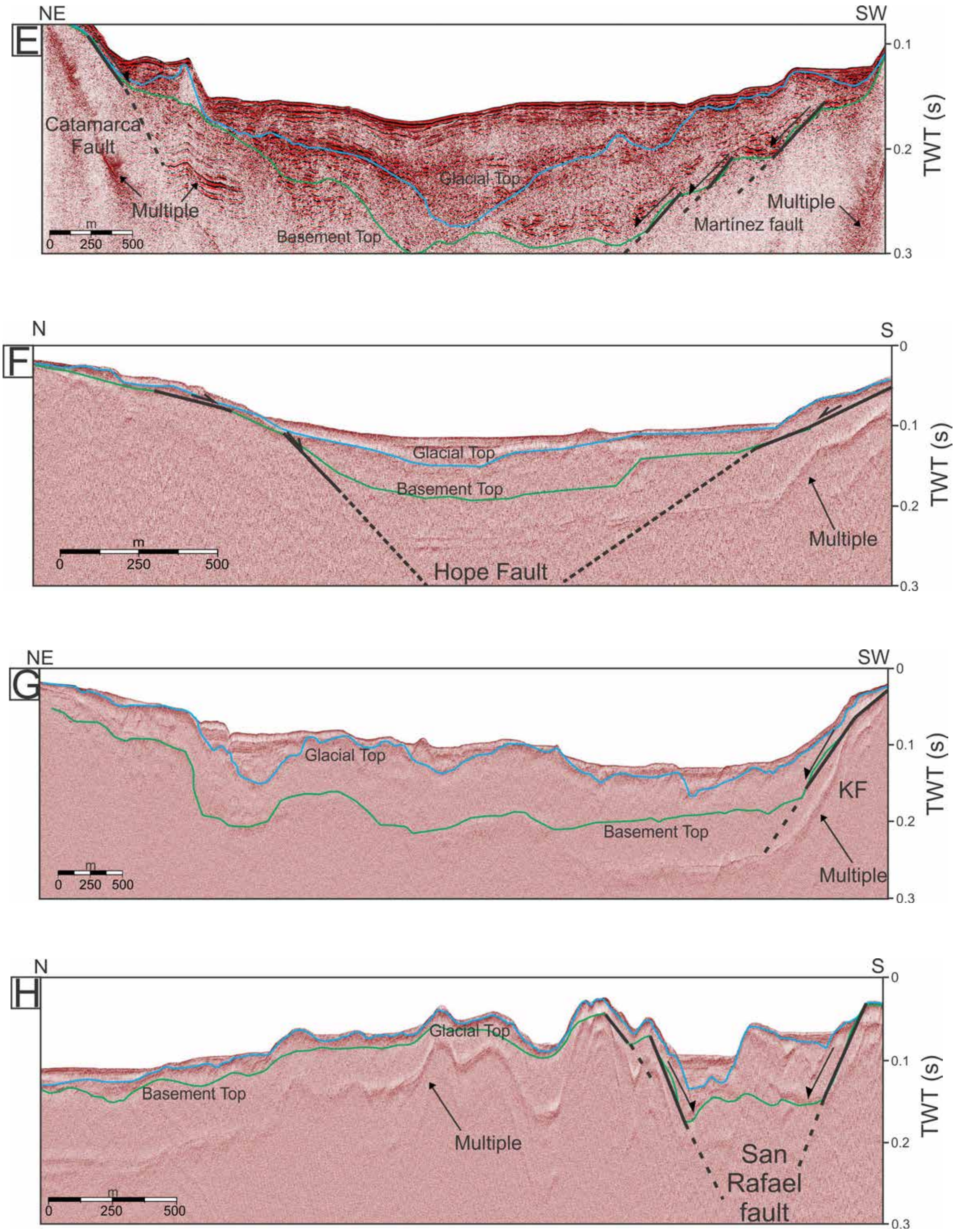

FIG. 6. Examples of seismic profiles. Top of the metamorphic basement (in green) and top of the glacial horizons (in blue) are shown. Major faults are indicated in black. **CF:** Catamarca Fault. 2KF: Knokeke Fault. **A**. Detail of seismic boomer section showing the main characteristics of the seismostratigraphic units identified. See location in figure 6D. **B-H.** Examples of Airgun (E) and Boomer **(B** to **D** and **F** to **H**) seismic profiles. See location in figure 5.

for this retreatment (Coronato *et al.,* 2009; Waldmann *et al.,* 2010a). In the Earliest Late Glacial (recessional phase 1) the ice expanded, covering all the current LF and originating the Tolhuin-Jeu Jepen frontal moraine (Coronato *et al.,* 2009). In the second recessional phase, the Fagnano glacier and its southern tributaries retreated leaving a series of lateral and central moraines within the LF eastern sector (A1-A5 of Waldmann *et al.,* 2010a) and a drumlin field along the LF southern shore (Coronato *et al.,* 2009). During the third recessional phase, the Fagnano glacier retreated to a stillstand or re-advance position at the Río Claro outlet originating a prominent frontal moraine (B1) and a proglacial lacustrine environment in the LF eastern sector (Waldmann *et al.,* 2010a). After that, the Fagnano glacier retreated (probably rapidly) leaving a series of terminal moraines (B2-B8) over the eastern part of the LF central main depocenter, probably related to temporary changes of weather conditions in the region (Waldmann *et al.,* 2010a). In the Latest Late Glacial the fourth recessional phase (3 of Coronato *et al.,* 2009) affected the westernmost part of LF. Different moraines (C7-C12, Isla Martínez, Isla Chilena; Fig. 2) have been related to this phase (Coronato *et al.,* 2009; Waldmann *et al.,* 2010a).

Finally, in mid-Holocene (about 6 ka), which marks the beginning of the Neoglacial in TdF (Unkel *et al.,* 2008; Waldmann *et al.,* 2010a), the Fagnano glacial lobe was restricted to the Cordillera Darwin high-mountain region, so the LF did not suffer any glaciation during this last period.

2.5. Previous data set on Lago Fagnano

During 2005-2006 a seismic survey and corings carried out within the LF provided the first data of the LF subsurface (Waldmann *et al.,* 2008, 2009, 2010a and 2010b). These studies allow recognizing three major seismic stratigraphic units (from bottom to top): **A.** a bedrock/basement complex unit; **B.** ice-contact/glacial deposits and **C.** glacio-lacustrine and lacustrine sediments. Waldmann *et al.* (2010a) recognized many frontal, lateral and central moraines related to multiple advances/stillstands of the Fagnano glaciers. The corings performed in the LF eastern sector showed more than 19 Holocene mass-wasting deposits most probably triggered by earthquakes related to the MFS (Waldmann *et al.,* 2010b). Waldmann *et al.* (2009) calculated two average background sedimentation rate (removing the mass-flow deposits) after a Holocene (7570±120 aBP) tephra (H1) derived from the Hudson volcano (Stern, 2008) found in the upper part of the unit C: 0.50 mm/yr in the western and 0.2-0.3 mm/yr in the center of the lake.

3. New data and methods

Between November 2009 and March 2010, 42 high-resolution single-channel seismic profiles (for a total of 179.5 km) were acquired using a Boomer seismic source and a single-channel, 10-m-long streamer (Fig. 5). Sampling rate was 0.005 ms, and the recording length 400 ms. Along-track horizontal resolution of 1 trace every 1.0 m was achieved shooting at 0.5 s interval (with an averaged ship speed of 4 knots). Data were first edited for noise traces, and a time-variant filtering and spike deconvolution were applied to produce the final version of the sections.

Previous seismic profiles acquired in LF by Waldmann (2008), and Waldmann *et al.* (2010a), were also used in this work. These authors collected simultaneously single-channel, high-resolution 3.5 kHz (pinger) and multichannel seismic data using 1 in^3 airgun (Waldmann *et al.,* 2008). The parameters used for data processing are reported in Waldmann *et al.* (2008). Between these two sets of seismic profiles, we used mainly the airgun-shooted seismic lines, because their higher sound penetration, providing information about the bedrock morphology. The bathymetry of the lake and the structural data from neighboring areas are taken from Zanolla *et al.* (2011).

The methodology consisted on the interpretation of the seismic database using the Kingdom Suite package (version 8.5). The seismostratigraphic units interpreted correspond to the previous units identified by Waldmann *et al.* (2010a).

To convert the two-way travel time of the high resolution profiles to depth, a water sound velocity of 1,432 m/s was used, following Zanolla *et al.* (2011). For the lacustrine, fluvial and glacial sediments a sound velocity of 1500 m/s was assigned following Waldmann *et al.* (2008, 2010a).

In order to generate more realistic grids, the geologic contacts between the different units outside the area of the LF were considered taking into account the correlation with the seismostratigraphic units. The horizon's grids were created by means of a Kriging method with a forcing factor along the E-W direction (Radius E-W: 54.500, Radius N-S: 40.000, angle: -5°), given the peculiar geometry of LF. Minor editing was applied to these grids in order to remove incoherent data. Finally, the GMT software (Wessel and Smith, 1991) was then used to generate all the figures.

4. Lago Fagnano subsurface geology

4.1. Seismostratigraphic units within Lago Fagnano

Three main seismostratigraphic units were interpreted in the seismic section: A, B and C (Fig. 6A). The unit A (basement) is characterized by discontinuous reflectors of medium to low amplitude and low frequency, which often result in a chaotic configuration. Usually, in the basement top a higher-amplitude reflector was observed. Unit B, interpreted as a glacial unit, developed over the basement unit, is mainly recognized by reflections with an internal configuration with SW prograding clinoforms, with low-to-high-amplitudes and variable discontinuity, which sometimes looks semi-transparent to chaotic. The uppermost part is characterized by a high-amplitude reflector. Unit C (glacio-lacustrine deposits) is easily identified by its medium-to-high amplitude, high frequency and highly continuous parallel reflectors. Occasionally, intervals of low-amplitude to transparent reflectors are found in the lower part of the unit. In figure 6 we present six seismic profiles showing the main structural and stratigraphic characteristics of LF, which will be later described.

The seismostratigraphic units were then correlated with the geologic units outcropping around the LF. Unit A was correlated with the Mesozoic-Paleogene units and unit B with the Quaternary sediments (glacial and fluvio-glacial) following Coronato *et al.* (2009) and Zanolla *et al.* (2011). Unit C (glacio-lacustrine deposits) was correlated with the shoreline of the lake taken from the Shuttle Radar Topography Mission Water Body Data. http://dds.cr.usgs.gov/srtm/version2_1/SWBD/SWBD_Documentation/SWDB_Product_Specific_Guidance.pdf.

4.2. Basement map of Lago Fagnano

In figure 7 we present the topography of the basement for the whole lake. The meaning of 'basement' as employed is related to the acoustic properties of the deepest and relatively continuous reflection recognizable in the study area. It may correspond to the top of both crystalline/metamorphosed rocks and sedimentary sequences, where they show a well-developed acoustic interface. It is worth to note that most of the reflections associated with the basement have been individuated from the water-gun seismic profiles (which are the most suitable profiles in this case because they illuminate deeper strata than the Boomer data), then the signals have been correlated throughout the entire seismic data grid.

The basement map shows three sub-basins: the eastern main sub-basin (Fig. 6B and C), the central main sub-basin (Fig. 6D and E; both previously described by Waldmann *et al.,* 2010a) and a third minor sub-basin, located in the LF western tip (Fig. 6F). Two basement highs of less than 90 m depth are located between the sub-basins. The eastern high is located just in correspondence of the Río Claro outlet (Fig. 6G) and the western one is located southwest of Punta Catamarca (Fig. 6H).

The eastern main sub-basin, south of Sierra Las Pinturas, is relatively small (*ca.* 21x5 km) and it reaches a depth of 373 m; the area deeper than 150 m is about 71 km^2. This sub-basin shows an E-W elongated shape with a steeper northern flank near the Río Turbio-Las Pinturas fault and a smooth southern flank (Fig. 6C).

The central main sub-basin is larger and shallower than the eastern one (Fig. 6D and E). It presents an elongated shape (*ca.* 44x3 km) and reaches a maximum depth of 215 meters. Almost 90 km^2 of the basement top in the lake basin is at a depth greater than 150 meters. In a N-S section, the western part of this sub-basin has a broadly symmetrical profile, which becomes slightly asymmetrical towards the east, near the Hope-Catamarca-Knokeke fault (Fig. 6D).

Between the eastern and central sub-basins, in correspondence with the Río Claro outlet, there is a structural high which rises at about 90 m depth below mean lake level. This feature has been interpreted as a pressure ridge or, alternatively, a transfer zone between the two main sub-basins constituting the LF, and controlled by the principal master faults (Lodolo *et al.,* 2003). In the western tip of the lake, there is a minor sub-basin (*ca.* 3.5x1.3 km) with a maximum depth of 128 m with an oblate shape and a slightly steeper northern slope (Fig. 7).

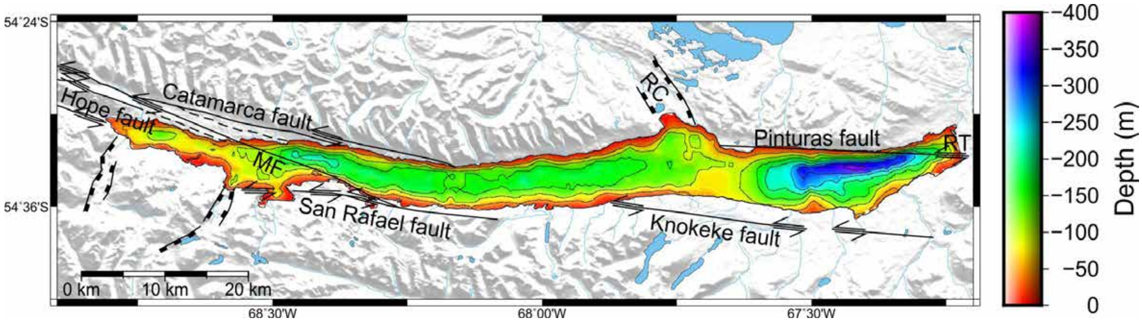

FIG. 7. Depth (in meters below the mean lake level) of the basement top. The depth was calculated assuming water sound velocity of 1,432 m/s and sediment sound velocity of 1,500 m/s. Contour lines (in black) are every 50 meters. **MF:** Martínez fault; **RT:** Río Turbio fault; **RC:** Río Claro fault.

Between the western minor sub-basin and the central main sub-basin there is a structural high (<100 m depth) that extends *ca.* 6 km with a WNW-ESE trend. We propose the existence of a structure (most likely a sinistral strike-slip fault) limiting both basins. This fault, here named 'Martínez', would run across the LF from Laguna Palacios, trough the Isla Martínez northern shore just to Punta Catamarca. It would merge the Hope-Catamarca-Knokeke fault at the north of Cerro Hope. This structure would explain the 100 m depth basement difference between the two sides of the fault (Fig. 6E) and the abrupt end of the sedimentary units. Preliminary anisotropic magnetic susceptibility studies in the Chilean sector of the LF (Espinoza *et al.,* 2011) along with GPS studies of crustal deformation (Mendoza *et al.,* 2011) located over the proposed trace of the Martínez fault, show WNW-ESE magnetic lineations and displacements that would confirm the fault direction. This structure would have had a structural control during the glacial recessional phase 4.

4.3. Map of the sedimentary cover

The data set allow reconstructing three isopach maps representing the total sedimentary thickness and the thickness of the two seismostratigraphic units already recognized by Waldmann *et al.* (2010a). The isopach sediment map (Fig. 8) shows a major deposition trend along the E-W axis of the LF with a gradual increase on the sedimentary thickness from nearly 100 m in the western part to more than 150 m in the eastern main sub-basin.

When we analyze the different areas of the LF, we see that over the eastern main sub-basin the sedimentation varies from nearly 0 m to almost 200 m. The zone of maximum deposition is located in a E-W direction parallel to the Río Turbio-Las Pinturas fault and gradually reduces towards south (Fig. 6C).

On the central main sub-basin, the thickness of the sedimentary cover ranges from 0 to *ca.* 100 m. The maximum thickness of the deposits is generally located towards the north (Fig. 6D). Two main depositional bodies are recognized. Both deposits have elongated shape and similar thickness. They differ in orientation: the eastern one has a general E-W trend and is located away from any major fault. The western deposit has an ENE-WSW orientation, parallel to the western segment of Hope-Catamarca-Knokeke fault.

In the area between the two main sub-basins (the Río Claro outlet), there is a relative important sedimentation (Fig. 6G), exceeding 100 meters, with the same NW-SE trend of the Río Claro normal faults. In the western tip of the FL, over the minor sub-basin, the sedimentary cover reaches over 50 m of thickness with a broadly circular shape.

The sedimentation rate within the LF is difficult to calculate due to the mass-wasting events (Waldmann *et al.,* 2010b) that modified the sedimentary thickness, and lack of a precise dating of the main events.

4.4. Map of the glacial sedimentary unit

The glacial isopach map (Fig. 9) shows that there is a major glacial accumulation that exceeds 100 m located in the eastern sector of LF. Two closed deposits are identified with thickness decreasing gradually northwards and separated by a zone where

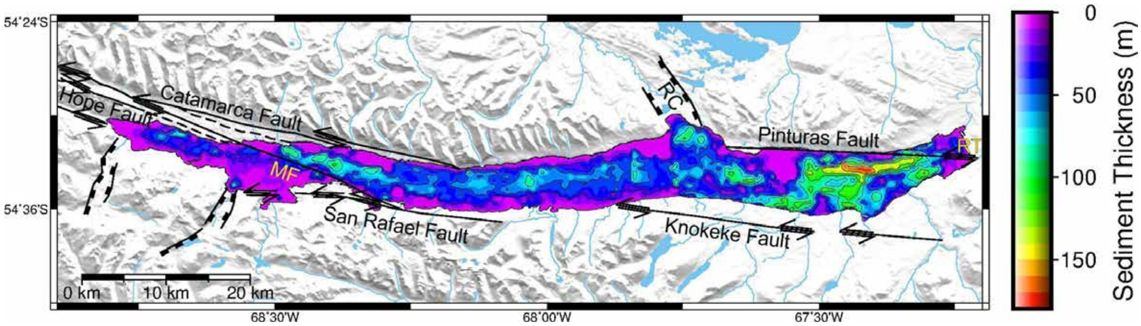

FIG. 8. Total sediment thickness map. The sediment thickness was calculated assuming a sediment sound velocity of 1500 m/s. Contour lines (in black) are every 50 m. **MF:** Martínez fault; **RT:** Río Turbio fault; **RC:** Río Claro fault.

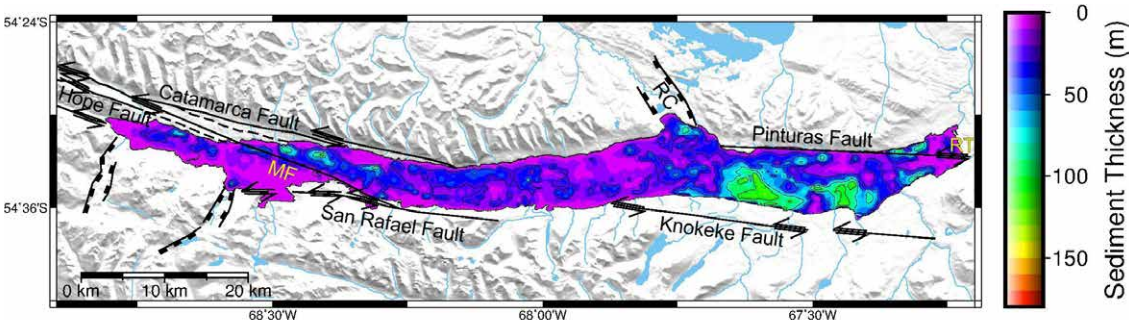

FIG. 9. Glacial isopach map. The sediment thickness was calculated assuming sediment velocity of 1500 m/s. Contour lines (in black) are every 50 meters. **MF:** Martínez fault; **RT:** Río Turbio fault; **RC:** Río Claro fault.

sedimentation is reduced. The western deposit is elongated in an E-W direction (10x5 km) while the eastern one has a circular shape in plain view (5x5 km). It is noteworthy that the seismic lines where this deposit was observed are restricted to the central sector of the LF (Fig. 2 of Waldmann *et al.,* 2010a). On the only seismic line that reaches the southern shore of the LF in this area (Fig. 6C) this important glacial deposit was not recognized. Therefore it is likely that the geometry of this deposit, both in extent and thickness, would be slightly smaller.

Northward, just in front of the Sierra Las Pinturas, two minor (less 100 m thick) broadly round-shaped (1 km diameter) deposits were recognized. These deposits are located over the northern flank of the lake, and were interpreted as lateral moraines (A3) by Waldmann *et al.* (2010).

Eastward, near the eastern tip of Sierra Las Pinturas and the Cerro Jeu Jepen, another a ENE-WSW elongated (about 3 km long) minor glacial deposit is located over the northern flanks of the LF (Fig. 6B). This deposit is located just to the south of the Río Turbio-Las Pinturas fault.

Towards the eastern tip of LF there are two NNW-SSE elongated glacial deposits. The eastern one is nearly 40 m thick and its size is 2x1 km, while the western one it is about half-size (1x0.5 km and 20 m thick). These deposits are located just north of the Río Turbio-Las Pinturas fault.

Near the Río Claro outlet, glacial deposits are widespread with three relative major accumulations (<50 m). The first one is located in the central part of LF slightly towards the southern shore of the lake. It has a broadly E-W elongated shape (5.5x2 km) with maximum thickness of *ca.* 50 m. The second major accumulation is located south of Las Pinturas fault and westward of the till deposits recognized onshore. It has an ENE-WSW elongated shape (*ca.* 2.5x1 km). The third accumulation, just in the Río Claro outlet is a WNW-ESE elongated (3.2x1.6 km) deposit with a maximum thickness of *ca.* 80 m. It is worth mentioning that this deposit is not observed in any seismic line. In the central part of LF, over the central main sub-basin, there are three deposits (> 50 m) located towards the northern flank of LF conforming a WNW-ESE trend parallel to the Hope-Catamarca-Knokeke fault system (Fig. 6D and E). The sediment thickness of these three deposits could be slightly smaller (about 30-40 m) since no seismic line cross their thicker zone. If so, these three deposits would form a single WNW-ESE elongated deposit of *ca.* 40 m of maximum thickness.

Near the Cerro Kranck and towards east, the glacial deposits are widespread along the LF. The sedimentary thickness is reduced (~ 20 m) and increases towards the northern shore. In addition, there are minor local maxima with an E-W elongated shape located in the central part of the lake (Fig. 9) that were interpreted as central moraines by Waldmann *et al.* (2010a).

In Bahía San Rafael, on the southern shore of LF there is a major triangular-shape deposit with more than 50 m of maximum thickness between two NNE-SSW-trending normal faults (Fig. 6B).

In the western tip of LF, in the minor sub-basin, the glacial sedimentary cover is reduced (<50 m) and slightly thicker to the north. It is likely that this deposit extends westward, but no seismic data cross this part of the lake.

4.5. Map of the lacustrine sedimentary unit

The main river inputs of LF are: Río Claro (between Sierra Las Pinturas and Sierra Beauvoir), Río Turbio (in the eastern shore), and Río Milna, Río Tuerto and Río Valdez (in the southern shore). The only outlet of LF is the Río Azopardo, located at the western tip of the lake.

The lacustrine isopach map (Fig. 10) shows that the accumulations are located preferentially along the E-W axis of LF and disappear towards the edges. In general, the sedimentary thickness reduces from east to west and is concentrated in bathymetric lows between glacial deposits (Fig. 6B, C, D, G and H). The most important accumulation is located in the eastern sector slightly towards the northern flank, near the Río Turbio-Las Pinturas fault (Fig. 6C) and has an E-W elongated shape (*ca.* 15x4 km) with a maximum accumulation of *ca.* 160 m.

On the central part of LF, within the central main sub-basin, the relatively poor lacustrine cover (<50 m) is accommodated along the central axis of the LF (Fig. 6D and E) with an E-W elongated shape (ca. 40x2.5 km). Between the two main sub-basins, there are three deposits located in the alignment of the Río Claro normal faults (Fig. 6G). The thickest one (*ca.* 50 m), next to the Río Claro outlet, has an E-W elongated shape (*ca.* 4.5x1.5 km) and rests over the northern flank of LF. The other two, along the central axis of the lake, are smaller (<40 m) and have a more rounded shape in plain view (*ca.* 5x3 km and 3x2 km).

On the westernmost part of the LF, there are three minor E-W elongated deposits (<25 m) located in the central part of LF. These deposits are 2 to 3 km in length and 1 to 1.5 km wide. Probably these deposits extend further west where there are no seismic data.

5. Discussion

The interpretation of the entire available seismic dataset for the LF, and the analysis of the geometry,

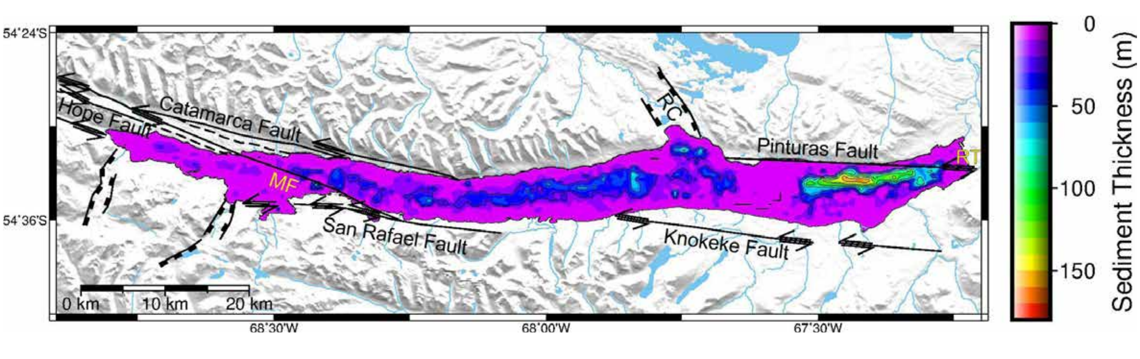

FIG. 10. Lacustrine isopach map. The sediment thickness was calculated assuming sediment sound velocity of 1500 m/s. Contour lines (in black) are every 50 meters. **MF:** Martínez fault; **RT:** Río Turbio fault; **RC:** Río Claro fault.

distribution, and thickness of the sedimentary units in the different sectors of the lake, allow us reconstructing the depositional processes, and the degree of influence that pre-existing tectonic features have generated on the sedimentary dynamics.

Either tectonic or glacial origin has been originally postulated for the origin of LF. The evidence that support the glacial origin is the glacial geoforms recognized along the margins and within the lake. On the other hand, the main evidence for a tectonic origin are: **1.** the negative Bouguer anomalies that extend beyond the LF and the glaciated area (Lodolo *et al.,* 2007), thus suggesting the presence of a regional E-W structure; **2.** the neotectonic activity registered by GPS stations and the seismicity (Mendoza *et al.,* 2011); **3.** active strike-slip fault systems identified along the margins of the lake. These evidences show that both processes (glacial and tectonics) occurred. Fig. 11, where bathymetry and basement topography of LF are compared, testify to the interplay between tectonic processes and glacial-related features.

The fact that the three sub-basins and the highs recognized in the basement show a good correlation in terms of location, shape, size and relative depth with the depocenters already shown in the bathymetric map of Zanolla *et al.* (2011) (Fig. 11), and the N-S asymmetry basement sections (perpendicular to the paleoglacier flow) indicate that the LF general morphology has been mainly controlled by tectonic features, as previously suggested by Lodolo *et al.* (2002b and 2003) and Lippai *et al.* (2004). Lodolo *et al.* (2003) and Esteban *et al.* (2012) describe depocenters developed within the principal displacement zone along the MFS onshore and offshore, respectively, in a manner similar to pull-apart asymmetric basins described by Aydin and Nur (1982), Ben-Avraham (1992) and Ben-Avraham and Zoback (1992). These basins are common in transform environments such as the Dead Sea Rift, El Pilar fault (off Venezuela) and Polochic-Motagua fault in Guatemala (*e.g.,* Lodolo *et al.,* 2009, Mann, 2007 for review): all of them are limited on one side by a sub-vertical master fault, and are characterized by an asymmetric sedimentary fan which thickens towards the main fault. In the eastern sector of LF, within the eastern main sub-basin, the basement top has a strong asymmetry, with its greater depth trend that parallels the strike of the Río Turbio-Las Pinturas fault (Fig. 6C).

The major role played by glacier in LF is evident. Significant glacial deposits located at the southern edge of the eastern main depocenter (and along the margin of LF) correspond to different ground moraines related to tributary glaciers from the Sierra Alvear (Fig. 6G and Waldmann *et al.,* 2010a). In addition, the glacial deposits located at the eastern tip of LF, based on their position and shape, can be related to the Tolhuin terminal moraine complex (Fig. 6B).

In the Río Claro outlet area, the basement structural high, possibly corresponding to a mid-basin ridge (Lodolo *et al.,* 2003), is located just eastward of the eastern limit of the Fagnano glacier accumulation area during the Last Glacial Maximum. This high is located next to the edge of the frontal moraine B1 where Waldmann *et al.* (2010a) interpret that the Fagnano glacier has stationed for an extended period after the Last Glacial Maximum. It is very likely that the structural high conditioned the location of the Fagnano glacier.

The central sector of the LF, between Cerro Kranck and the Río Claro outlet (eastern sector of the central main sub-basin), is the area where the more intense glacial activity occurred probably erasing the different tectonic features that might have existed. This is evidenced by the polished slopes and truncated spurs of the mountains flanks, and the N-S section through the metamorphic basement and the topography adjacent to the lake that describes a symmetrical profile (Fig. 6D). The erosive features can be related to the N-S compressional regime as described by the GPS data (Mendoza *et al.,* 2011).

To the west, between Cerro Kranck and Punta Catamarca (western sector of the central main sub-basin), the basement is slightly asymmetrical, with its deepest zone towards the Hope-Catamarca-Knokeke fault, probably reflecting the development of an incipient asymmetrical pull-apart basin.

In the Bahía San Rafael and Bahía Grande, along the southern margin of the LF, a small basement depocenter trending broadly E-W, parallel to the San Rafael fault, and with major accumulations within the depocenter, would indicate a negative flower structure and an asymmetrical pull-apart basin (Fig. 6H).

In the western tip of LF, within the minor sub-basin, the major axis of this basement depocenter aligns with the Hope fault. In a N-S section, the basement is slightly asymmetric with its deepest part towards the north. The sediment accumula-

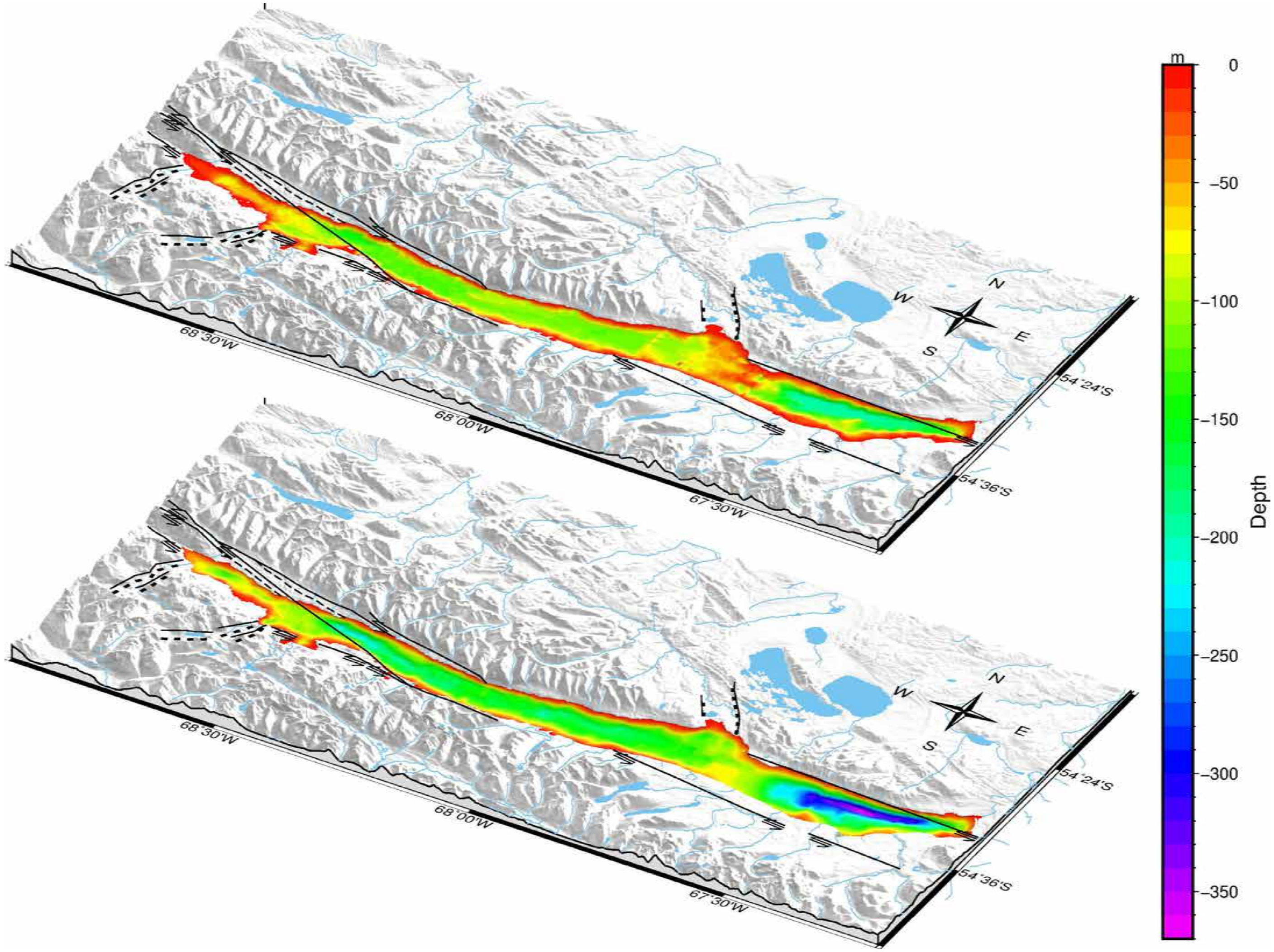

FIG. 11. 3-D perspective images of the bathymetry (top) and top basement (bottom) of Lago Fagnano (measured in meters below the mean lake level), superimposed onto the Digital Elevation Model.

tion is thicker in that direction. We interpret this depocenter as a negative flower structure related to the Hope fault.

Summarizing, the Lago Fagnano was mainly controlled by tectonic processed that shaped its general morphology. The glacial process played a secondary control, modeling the previous tectonic features.

The distribution of most lacustrine sediments filling the topographic lows left by glacial deposits can be indirectly linked to the seismic activity of the MFS. Mass-wasting events triggered by earthquakes, as described by Waldmann *et al.* (2010b) for the eastern sector of the LF, remobilized the sediments to the deeper zones. The only exception is the accumulation located on the LF northern flank at the Río Claro outlet, which is composed of fluvial deposits. The trend of increasing thickness of the lacustrine unit to the east could be related to the gradual establishment of lacustrine conditions from east to west as the Fagnano glacier retreated, as suggested by Waldmann *et al.* (2010a).

Evidence of Neotectonic activity has been documented around LF (Menichetti *et al.,* 2007b). In the eastern part of the lake linear truncation of river meanders, left lateral drag of river valley and hanging valley evidenced the Quaternary activity of strike-slip faults. During the 1949 earthquake on the eastern bank of the Lago Fagnano shore a W-E scarp of about 1 m formed. The kinematic analysis of fault populations in the area shows a prevalent left-lateral transtensional component (Menichetti *et al.,* 2001). In the LF western area, another E-W scarp of few meters shows a transtensional pattern deformation, including fault gouge.

Based on the structural data observed in the outcrops around the LF and the geophysical data, we proposed that the LF is composed by 4 pull-apart sub-basins developed along a releasing stepover (Fig. 12). The sub-basin 1 corresponds to the western bathymetric depocenter, the sub-basins 2 and 3 with the central depocenter and the sub-basin 4 with the eastern one. Aydin and Nur (1982) observed that the pull-apart basins have a length / width empirical relationship of 3:1. The high length/width relationship (14.7) of the central depocenter supports the idea that it consist of 2 pull-apart sub-basins. This differentation is based on the differences between the western and eastern sector of the central depocenter previously described. Evidence of the subdivision within the lake basin would have been erased by the glacial activity.

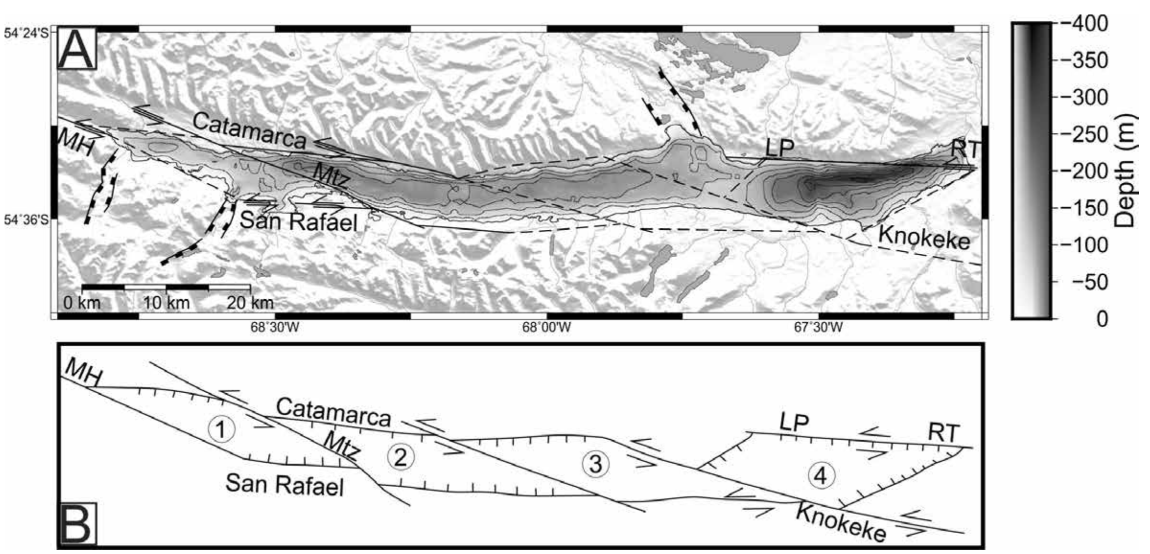

FIG. 12. **A.** Major faults (observed and inferred) of Lago Fagnano area superimposed onto Digital Elevation Model (SRTM v. 4.1.; Farr *et al.,* 2007) and basement top within the lake. **B.** Structural sketch of Lago Fagnano composed by 4 pull-apart basins made from the analyzed data. **LP:** Las Pinturas fault; **MH:** Monte Hope; **Mtz:** Martínez Fault; **RT:** Río Turbio fault.

6. Conclusions

We have analyzed the geometry, distribution and thickness of the sedimentary units filling the LF basin, and related them with the pre-existing tectonic lineaments characterizing the depression. The activity of the MFS, with a stepover releasing geometry, generated 4 pull-apart basins and mainly transtensional structures along the strike of the fault system. In the eastern sector of the lake, a major deep (373 m basement depth) asymmetric pull-apart basin (*ca.* 21x5 km) associated with the fault Las Pinturas-Rio Turbio fault was developed, while in the outlet of the Río Claro a small pressure ridge was generated.

From the Río Claro to Punta Catamarca, another basin was developed (*ca.* 44 km long x 3 km wide and 150 m deep). In the eastern sector, between the Río Claro and Cerro Kranck, the tectonic activity was less pronounced, probably because the presence of a transfer zone, while in the western sector, westward of Cerro Kranck, an asymmetric pull-apart basin was developed in relationship to the Hope-Catamarca-Knokeke fault.

At the LF western tip, an even smaller basin (*ca.* 3.5 km long x 1.3 km wide and 128 m deep) was developed probably related to the transtensional activity of the Hope fault which generated a negative flower structure.

Sedimentary cover is widespread along the LF, being thicker over the basement deepest zone and with a gradually thickening pattern to the east where it reaches a sedimentary thickness of more than 150 m within the eastern pull-apart basin. The major accumulations have elongated shape and filling up the asymmetric pull-apart basins related to the Hope-Catamarca-Knokeke and Río Turbio-Las Pinturas fault.

Glacial deposits are present over the entire LF, but preferentially concentrated along the SE margin next to the onland glacial deposits (>100 m thick). Another less important accumulation, also related to onshore deposits, is present in the NW margin (*ca.* 75 m), near the Río Claro outlet (*ca.* 40 m), and in the eastern tip of LF (*ca.* 40 m). In the central and western sector of LF, E-W elongated deposits which correspond to central moraines are present. The lacustrine sediments are preferentially localized along the E-W axis of the lake filling topographic lows. The maximum deposits thickness (*ca.* 150 m) is located within the eastern pull-apart basin, along and E-W trend parallel to the Río Turbio-Las Pinturas fault.

Acknowledgments

We acknowledge those people who contributed with field work in Tierra del Fuego: J.L. Hormaechea, G. Connon, L. Barbero and C. Ferrer of the EARG for their support during data acquisition in the field, M. Grossi (OGS) for seismic acquisition, and Parques Nacionales of Argentina by providing facilities for the survey of the National Park of Tierra del Fuego. Funds for the November 2009 campaign in Lago Fagnano were provided by the Italian Foreign Ministry. Funds for this study were partly provided by the Italian Foreign Ministry and the MinCyt 'La Agencia' PICT 2007-00106 projects and from Consorzio Universitario Italiano per l'Argentina (CUIA). We are grateful for the thorough and constructive reviews made by G. Yáñez and F. Audemard which greatly improved the original manuscript.

References

Angelier, J.; Goguel, J. 1979. Sur une méthode simple de determination des axes principaux des contraintes por une population de failles. Comptes Rendus Royale Académie Sciences de Paris 288: 307-310.

Aydın, A.; Nur, A. 1982. Evolution of pull-apart basins and their scale independence. Tectonics 1: 91-105. doi: 10.1029/TC001i001p00091.

Ben-Avraham, Z. 1992. Development of asymmetric basins along continental transform faults. Tectonophysics 215: 209-220.

Ben-Avraham, Z.; Zoback, M.D. 1992. Transform-normal extension and asymmetric basins: An alternative to pull-apart models. Geology 20: 423-426.

Borrello, A.V. 1969. Los geosinclinales de la Argentina. Anales de la Dirección Nacional de Geología y Minería 14: 1-188. (Argentina).

Bujalesky, G.; Heusser, C.; Coronato, A.; Roig, C.; Rabassa, J. 1997. Pleistocene glaciolacustrine sedimentation at Lago Fagnano, Andes of Tierra del Fuego, Southernmost South America. Quaternary Science Review 16: 767-778.

Caldenius, C. 1932. Las glaciaciones Cuaternarias en Patagonia y Tierra del Fuego. Geografiska Annaler 14: 1-164.

Camacho, H.H. 1967. Las transgresiones del Cretácico superior y Terciario de la Argentina. Revista Asociación Geológica Argentina 22: 253-254.

Caminos, R.; Haller, M.; Lapido, O.; Lizuain, A.; Page, R.; Ramos, V. 1981. Reconocimiento geológico de los Andes Fueguinos. Territorio Nacional de Tierra del Fuego. *In* Congreso Geológico Argentino, No. 8, 3: 759-786. San Luis.

Cerredo, M.E.; Remesal, M.B.; Tassone, A.; Lippai, H. 2005. The shoshonitic suite of Hewhoepen pluton, Tierra del Fuego, Argentina. *In* Congreso Geológico Argentino, No. 16, Actas I: 539-544. La Plata.

Cerredo, M.E.; Tassone, A.; Rapalini, A.; Hervé, F.; Fannin, X. 2011. Campanian magmatism the Fuegian Andes: New SHRIMP age of Jeujepen pluton. Argentina. *In* Congreso Geológico Argentino, No. 18, Abstracts in CD. 2 p. Neuquén.

Coronato, A.; Seppala, M.; Ponce, F.J.; Rabassa, J. 2009. Glacial Geomorphology of the Pleistocene Lake Fagnano ice lobe, Tierra del Fuego, southern South America. Geomorphology 112: 67-81.

Cunningham, W.D. 1993. Strike-slip faults in the southernmost Andes and the development of the Patagonian orocline. Tectonics 12 (1): 169-186.

Cunningham, W.D. 1995. Orogenesis at the southern tip of the Americas: the structural evolution of the Cordillera Darwin metamorphic complex, southernmost Chile. Tectonophysics 244: 197-229.

Dalziel, I.W.D. 1989. Tectonics of the Scotia Arc, Antarctica. Field Trip Guide T180. American Geophysical Union: 206 p. Washington, D.C.

Esteban, F.D.; Tassone, A.; Menichetti, M.; Cerredo, M.E.; Rapalini, A.E.; Lippai, H.; Vilas, J.F. 2009. Suscettività magnetica e assetto strutturale nelle Ande in Tierra del Fuego. Rendiconti Online Società Geologica Italiana 5: 80-83.

Esteban, F.D.; Tassone, A.; Menichetti, M.; Rapalini, A.E.; Remesal, M.B.; Cerredo, M.E.; Lippai, H.; Vilas, J.F. 2011. Magnetic fabric and microstructures across the Andes of Tierra del Fuego, Argentina. Andean Geology 38 (1): 64-81.

Esteban, F.D.; Tassone, A.; Lodolo, E.; Menichetti, M. 2012. The South America-Scotia plate boundary from 67°W to 56°W (Southermost Atlantic ocean). Rendiconti Online Società Geologica Italiana 22: 76-79.

Espinoza, M.; Poblete, F.; Arriagada, C.; Roperch, P. 2011. Resultados preliminares de un estudio de anisotropía de susceptibilidad magnetica, Tierra del Fuego, Chile. Latinmag Letters-An Electonic Journal. http://www.geofisica.unam.mx/LatinmagLetters/LL11-0102P/D/D30-Espinoza.pdf.

Farr, T.G.; Rosen, P.A.; Caro, E.; Crippen, R.; Duren, R.; Hensley, S.; Kobrick, M.; Paller, M.; Rodríguez, E.; Roth, L.; Seal, D.; Shaffer, S.; Shimada, J.; Umland, J.; Werner, M.; Oskin, M.; Burbank, D.; Alsdorf, D. 2007. The Shuttle Radar Topography Mission. Review Geophysics 45 (2): RG2004.

Fuenzalida, R.H. 1972. Geological correlation between the Patagonian Andes and the Antarctic Peninsula and some tectonic implications. Master's thesis (Unpublished), Stanford University: 75 p. Stanford.

Heusser, C.J. 1998. Deglacial paleoclimate of the American sector of the Southern Ocean: Late Glacial-Holocene records from the latitude of Canal Beagle (55°S), Argentine Tierra del Fuego. Palaeoecology 141: 277-301.

Klepeis, K.A. 1994. The Magallanes and Deseado fault zones: Major segments of the South American-Scotia transform plate boundary in southernmost South America, Tierra del Fuego. Journal Geophysical Research 99: 22001-22014.

Lippai, H.; Lodolo, E.; Tassone, A.; Hormaechea, J.L.; Menichetti, M.; Vilas, J.F.; TESAC Party, 2004. Morpho-structure of Lago Fagnano (Tierra del Fuego) and adjacent areas. Bollettino di Geofísica Teorica ed Applicata 45 (2): 142-144.

Lodolo, E.; Menichetti, M.; Tassone, A.; Sterzai, P. 2002a. Morphostructure of the central-eastern Tierra del Fuego Island from geological data and a remote-sensing images. EGS Stephan Mueller Special Publication Series 2: 1-16.

Lodolo, E.; Menichetti, M.; Tassone, A.; Geletti, R.; Sterzai, P.; Lippai, H.; Hormaechea, H.L. 2002b. Researches target a continental transform fault in Tierra del Fuego. EOS Transactions American Geophysical Union 83 (1): 1-3. doi: 10.1029/2002EO000001.

Lodolo, E.; Menichetti, M.; Bartole, R.; Ben-Avraham, Z.; Tassone, A.; Lippai, H. 2003. Magallanes-Fagnano continental transfom fault (Tierra del Fuego, southernmost South America). Tectonics 22 (6): 1076. doi: 10.1029/2003TC001500.

Lodolo, E.; Lippai, H.; Tassone, A.; Zanolla, C.; Menichetti, M.; Hormaechea, J.L. 2007. Gravity map of the Isla Grande de Tierra del Fuego, and morphology of Lago Fagnano. Geologica Acta 4: 307-314.

Lodolo, E.; Menichetti, M.; Guzmán-Speziale, M.; Giunta, G.; Zanolla, C. 2009. Deep structural setting of the North American-Caribbean plate boundary in eastern Guatemala. Geofísica Internacional 48 (3): 263-277.

Mann, P. 2007. Global catalogue, classification and tectonic origins of restraining- and releasing bends on active and ancient strike-slip fault systems. *In* Tectonics of Strike-Slip Restraining and Releasing Bends: Geological Society (Cunningham, W.D.; Mann, P.;

editors), Special Publication 290: 13-142. London. doi: 10.1144/SP290.2.

Mendoza, L.P.O. 2008, Densificación del Marco de Referencia Terrestre ITRF y determinación de movimientos de la corteza en la Tierra del Fuego. Resultados del procesamiento de 14 años de observaciones GPS. Tesis doctoral, Universidad Nacional de La Plata: 154 p. La Plata.

Mendoza, L.; Richter, A.; Hormaechea, J.L.; Perdomo, R.; Del Cogliano, D.; Dietrich, R.; Fritsche, M. 2010. Do crustal deformations observed by GPS in Tierra del Fuego (Argentina) reflect glacial-isostatic adjustment? Cryosphere Discussions 4 (3): 1635-1645.

Mendoza, L.; Perdomo, R.; Hormaechea, J.L.; Del Cogliano, D.; Fritsche, M.; Richter, A.; Dietrich, R. 2011. Present-day crustal deformation along the Magallanes-Fagnano Fault System in Tierra del Fuego from repeated GPS observations. Geophysical Journal International 184: 1009-1022.

Menichetti, M.; Lodolo, E.; Tassone, A.; Geletti, R. 2001. Neotectonics at the continental Transform boundary of the South America-Scotia plates: the Magallanes-Fagnano fault system. Terra Antartic Publ ‘Antartic Neotectonic’ workshop: 55 p. Siena.

Menichetti, M.; Lodolo, E.; Tassone, A.; Hormaechea, J.L.; Lippai, H. 2007a. Geologia dell’area del Lago Fagnano in Terra del Fuoco (Sud America). Rendiconti Online Società Geologica Italiana 4: 251-254.

Menichetti, M.; Tassone, A.; Flores, J. 2007b. Neotectonics and seismotectonics of the Tierra del Fuego region. Geosur 2007 Abstracts 127: p. 100.

Menichetti, M.; Lodolo, E.; Tassone, A. 2008. Structural geology of the Fuegian Andes and Magellanes fold-and-thrust beld-Tierra del Fuego Island. Geologica Acta 1: 19-42.

Peroni, J. 2012. Modelado geofísico-geológico de plutones en las Islas Grande de Tierra del Fuego (Argentina) y Navarino (Chile). Tesis doctoral (Inédito), Universidad de Buenos Aires: 430 p. Buenos Aires.

Peroni, J.; Tassone, A.; Lippai, H.; Menichetti, M.; Lodolo, E.; Vilas, J.F. 2007. Geophysical modeling of the Kranck pluton. Tierra del Fuego. Argentina. *In* International Geological Congress on the Southern Hemisphere (Geosur 2), Abstracts book: p. 122. Santiago.

Peroni, J.; Tassone, A.; Menichetti, M.; Lippai, H.; Lodolo, E.; Vilas, J.F. 2008. Geologia e geofisica del plutone Kranck (Lago Fagnano, Tierra del Fuego, Argentina). Rendiconti Online della Società Geologica Italiana 1: 132-136.

Rabassa, J.; Coronato, A.; Martínez, O. 2011. Late Cenozoic glaciations in Patagonia and Tierra del Fuego: an updated review. Biological Journal of the Linnean Sociecty 103: 316-335.

Rossello, E.A. 2005. Kinematics of the Andean sinistral wrenching along the Fagnano-Magallanes Fault Zone (Argentina-Chile Fuegian foothills). *In* International Symposium of Andean Geodynamics, No. 6, Extended Abstracts: 623-626. Barcelona.

Stern, C.R. 2008. Holocene tephrochronology record of large explosive eruptions in the Southernmost Patagonian Andes. Bulletin of Volcanology 70: 435-454.

Sugden, D.E.; Bentleyt, M.J.; Fogwill, C.J.; Hulton, N.R.J; McCulloch, R.D.; Purves, R.S. 2005. Late-glacial glacier events in southernmost South America: A blend of ‘northern’ and ‘southern’ hemispheric climatic signals? Geografiska Annaler, Series A. Physical Geography 87 (2):273-288.

Tassone, A.; Lippai, H.; Lodolo, E.; Menichetti, M.; Comba, A.; Hormaechea, J.L.; Vilas, J.F. 2005. A geological and geophysical crustal section across the Magallanes-Fagnano fault system in Tierra del Fuego. Journal of South American Earth Sciences 19: 99-109.

Tassone, A.; Santomauro, M.G.; Menichetti, M.; Cerredo, M.E.; Lodolo, E.; Remesal, M.B.; Lippai, H.; Hormaechea, J.L.; Vilas, J.F. 2011. ERT imaging of a shallow basin: Easetern Lago Fagnano, Tierra del Fuego, Argentina. Bolletino di Geofísica Teorica ed Applicata 52 (1): 9-21.

Unkel, I.; Björck, S.; Wohlfarth, B. 2008. Deglacial environmental changes on Isla de los Estados (54.4°S), southeastern Tierra del Fuego. Quaternary Science Review 27: 1541- 1554.

Waldmann, N. 2008. Late Quaternary environmental changs in Lago Fagnano, Tierra del Fuego (54°S): Reconstructing Sedimentary Processes, Natural Hazards and Paleoclimate. Tesis doctoral (Unpunblished), Universite de Genève: 150 p. Genève.

Waldmann, N.; Ariztegui, D.; Anselmetti, F.S.; Austin, J.A. Jr.; Dunbar, R.B.; Moy, C.M.; Recasens, C. 2008. Seismic stratigraphy of Lago Fagnano sediments (Tierra del Fuego, Argentina) - a potential archive of Paleoclimatic change and tectonic activity since the Late Glacial. Geologica Acta 6: 101-110.

Waldmann, N.; Ariztegui, D.; Anselmetti, F.S.; Austin, J.A. Jr; Moy, C.M.; Stern, C.; Recasens, C.; Dunbar R.B. 2009. Holocene climatic fluctuations and positioning of the Southern Hemisphere westerlies in Tierra del Fuego (54°S), Patagonia. Journal Quaternary Sciences 25 (7): 1063-1073. doi: 10.1002/jqs.1263.

Waldmann, N.; Ariztegui, D.; Anselmetti, F.S.; Coronato, A.; Austin, J.A.Jr. 2010a. Geophysical evidence of multiple glacier advances in Lago Fagnano (54°S), southernmost Patagonia. Quaternary Science Review 29: 1188-1200.

Waldmann, N.; Anselmetti, F.S.; Ariztegui, D.; Austin, J.A.Jr; Pirouz, M.; Moy, C.M.; Dunbar, R. 2010b. Holocene mass-wasting events in Lago Fagnano, Tierra del Fuego (54°S): implications for paleoseismicity of the Magallanes-Fagnano transform fault. Basin Research 23 (2): 171-190. doi: 10.1111/j.1365-2117.2010.00489.x.

Wessel, P.; Smith, W.H.F. 1991. Free software helps map and display data. EOS Transactions American Geophysical Union 72 (41): 441-446.

Zanolla, C.; Lodolo, E.; Lippai, H.; Tassone, A.; Menichetti, M.; Baradello, L.; Grossi, M.; Hormaechea, H.L. 2011. Bathymetric map of Lago Fagnano (Tierra del Fuego Island). Bollettino di Geofisica Teorica ed Applicata 52 (1): 1-8.

Manuscript received: May 9, 2013; revised/accepted: Marzo 6, 2014; available online: Marzo 6, 2014.